Stability of NaSICON-type $Li_{1.3}Al_{0.3}Ti_{1.7}P_3O_{12}$ in aqueous solutions

Spencer D. Jackman*, Raymond A. Cutler

Department of Materials Science and Engineering, University of Utah, Salt Lake City, UT 84112, USA

HIGHLIGHTS

► LATP operated in aqueous $LiCOOCH_3$ for >600 h at 25 mA cm^{-2} without failure.
► Cathodic corrosion of LATP in high pH (>12) under electrochemical conditions.
► High biaxial strength (191 MPa) when measured in mineral oil.
► Severe degradation of strength in presence of water and Na$^+$ ions.
► D.c. conductivity of 1.1–1.8 mS cm^{-1} at 40 °C measured in aqueous Li salt solutions.

ARTICLE INFO

ABSTRACT

The chemical and electrochemical stability of high-purity lithium aluminum titanium phosphate (LATP) as a solid state electrolyte and physical separator in aqueous electrochemical cells was evaluated using LiOH, LiCl, $LiNO_3$, and $LiCOOCH_3$ salts as the Li source. LATP, with formula $Li_{1.3}Al_{0.3}Ti_{1.7}P_3O_{12}$, was found to be most stable between pH 8–9, with the longest cell operating continuously at 25 mA cm^{-2} for 625 h at 40 °C in $LiCOOCH_3$. Biaxial strength was 191 ± 11 MPa when tested in mineral oil, 144 ± 13 MPa as measured in air, and 26 ± 7 MPa after exposure to deionized water, suggesting that LATP undergoes stress-corrosion cracking. After exposure to LiOH, the strength was 76 ± 19 MPa. The decrease in strength was observed despite there being no measurable change in a.c. impedance spectra, x-ray diffraction, or sample mass, suggesting phosphate glasses at grain boundaries. At pH values outside of the 7–10 range, eventual membrane degradation was observed in all aqueous systems under electrochemical conditions. While LATP was surprisingly resistant to static corrosion in a hot, aqueous LiOH solution, electrochemical degradation was observed at the cathode due to subsurface pitting. Strength measurements were more instructive than impedance measurements in detecting this degradation.

© 2012 Elsevier B.V. All rights reserved.

1. Introduction

There is an ongoing research and development effort to develop a Li ion battery that exhibits high energy capacity and cyclability while overcoming the limited temperature range and safety concerns inherent to organic electrolyte and polymer-based batteries that currently dominate the market [1–3]. This is of specific concern for large scale batteries used in electric vehicles [4–7] and industrial scale power storage [8,9]. Li et al. [10] introduced the first aqueous rechargeable Li ion battery in 1994 which would have a clear advantage over their non-aqueous counterparts in terms of being safer, cheaper, and more environmentally friendly [11–15]. Since then, a significant effort has focused on an aqueous alternative to the current battery configuration using water stable Li ion conductors as the positive and/or negative electrodes [16–23].

Due to the narrow electrochemical stability range of water, electrode materials for an aqueous Li ion battery must be chosen carefully. Lithium titanium phosphate (LTP), with chemical formula $LiTi_2P_3O_{12}$, is a Li ion conducting material from the sodium zirconium phosphate (NZP) family being considered as a negative electrode material in aqueous Li ion batteries [16,24–28]. It has an open-circuit potential of 2.5 V with respect to lithium metal, which is below the 2.6 V decomposition potential of aqueous electrolytes at standard temperature and pressure [16] and has good electrochemical stability in water over a pH range of 7–9 [16,28]. However, LTP has significantly lower conductivity than the Al doped lithium aluminum titanium phosphate (LATP) first reported by Aono et al. [29] with composition $Li_{1.3}Al_{0.3}Ti_{1.7}P_3O_{12}$. LATP possesses adequate ionic conductivity in an aqueous electrochemical cell to be used in many electrochemical applications, including as an electrode material in

aqueous Li ion batteries and as a Li transporting separator for aqueous stream purification and concentration [30–32]. However, it has often been reported in the literature that LATP is not water stable, and although stability has been enhanced with slight additions of Si at the P site according to $Li_{1+x+y}Al_xTi_{2-x}Si_yP_{3-y}O_{12}$, where x is ~0.25 and y is 0.1–0.3 [33–35], these materials still exhibited poor stability in water and degraded in alkaline solutions, namely LiOH, after even short exposure times [36–38].

If long-term stability of LATP could be demonstrated under electrochemical conditions in aqueous media, especially in inexpensive solutions such as LiOH, it could lead to several applications, including aqueous Li ion batteries. In many studies, LATP has been determined to be stable or instable in a given media due solely to changes in XRD patterns and/or a.c. impedance spectra. The objectives of the present study were to: 1) compare the d.c. conductivity of LATP in various lithium salts, at the same Li^+ content, in aqueous solutions tested at 40 °C, 2) use strength measurements on ceramic membranes as a means of monitoring electrochemical degradation, and 3) identify parameters which allow LATP to be used in aqueous environments.

2. Experimental

2.1. Characterization of physical properties

All testing was performed on high-purity LATP ($Li_{1.3}Al_{0.3}Ti_{1.7}P_3O_{12}$) specimens [30] that were obtained from Ceramatec, Inc. (Salt Lake City, Utah). Crystalline phases present were identified using an X-ray diffractometer (Philips model PW3040). Scans were conducted with Cu K_α radiation over a 2θ range of 15–75° using a step size of 0.02° and a 0.05 s dwell time. Density based on Archimedes' principle was measured in isopropyl alcohol. The microstructure was examined using a scanning electron microscope (JEOL model JSM-5900LV SEM).

2.2. Static corrosion measurements

Pellets with a 15 mm diameter and 5 mm thickness were used to measure the corrosion rate of LATP as a function of time in saturated aqueous LiOH at 65 °C (3 pellets) and at the boiling point, or $T \sim 105$ °C (5 pellets). Pellets at 65 °C were placed in an HDPE bottle with 500 ml of solution and the change in mass of the pellets was recorded after 1, 4, and 7 week intervals. Pellets at 105 °C were continuously boiled in 1000 ml of solution inside a glass bulb connected to a reflux unit with a water-chilled condenser tube. Pellet mass loss/gain measurements were taken at 1 and 4 week intervals. Corrosion rate was taken to be the mass loss/gain in mg per cm^2 per 100 h.

2.3. Ionic conductivity measurements

2.3.1. A.c. conductivity
Pellets used in static corrosion testing in boiling LiOH were used for solid state a.c. impedance measurements before and after 4 weeks of exposure to boiling LiOH. Gold electrodes were sputtered (Fullam EffaCoater) on both sides of the pellets that had been exposed to the LiOH, ultrasonicated in isopropyl alcohol and deionized water, and then dried. A 'best fit circle' technique was used to analyze Nyquist plots to determine the bulk, grain boundary, and total ionic conductivity. A.c. impedance measurements were also taken on a 25 mm diameter by 1 mm thick membrane used for d.c. testing in an aqueous $LiNO_3$ solution to investigate any change in a.c. impedance as a function of operating time. In this case, the gold electrodes were sputtered onto the membrane before d.c. testing and the deposition was confirmed to

be porous via scanning electron microscopy. The membrane was cleaned according to the procedure described above before a.c. measurements. All measurements were made with a spectrometer (Solartron model SI 1260 Impedance/Gain-Phase) at an a.c. amplitude of 40 mV over a frequency range of 100 Hz to 10 MHz at room temperature.

2.3.2. D.c. conductivity
Electrochemical testing was conducted using the cell setup shown in Fig. 1 to determine the performance and conductivity of the 25 mm diameter by 1 mm thick LATP membranes for 30 h under d.c. conditions. The test cell has EPDM gaskets between the spacers and membrane scaffold and o-rings to seal and isolate the anode and cathode compartments. Using LiOH, LiCl, $LiNO_3$, and $LiCOOCH_3$ as lithium salts for the aqueous electrolytes, solutions were maintained at approximately 2.0 wt% Li content regardless of the salt used. The Na concentration in each solution and the deionized water used to make the solutions was measured using inductively coupled plasma (ICP) analysis. Tests were conducted at 40 °C with a current density of 25 mA cm^{-2} using a Pt anode and Ni cathode, with a peristaltic pump being used to maintain a flow rate of ~500 ml min^{-1} through polypropylene tubing. Commercial software (Labview) was used to collect the voltage and current readings at 30 s intervals throughout the duration of each test. Tests were conducted with electrolytes in one of three possible configurations: 1) common flask—anolyte and catholyte drawn from and returned to a common source, 2) separate flask—anolyte and catholyte compartments kept separate from each other, or 3) separate flask, pH controlled—same as separate flask but with pH maintained between desired values. The voltage due to reactions at the electrodes was measured in situ, but with no membrane separating the cathode and anode compartments to obtain a 'blank' reading. This was used to isolate the resistance across the membrane, including interfacial resistances, for d.c. conductivity calculations.

2.4. Strength measurements

The biaxial strength of specimens used in this study was determined using a universal testing machine (Instron model 5566) with a 1 kN load cell for the standard ring-on-ring test (ASTM C1499-04). The support structure had a radius on the compression side of 6.5 mm and a radius on the tension side of 9.5 mm. A load was applied via a steel ball which was pressed against the top ring fixture through lowering a pushing rod attached to the testing machine at 0.5 mm min^{-1} with data collected every 50 ms. Tests were conducted in air, mineral oil, deionized water, and aqueous solutions of LiOH, LiCl, $LiNO_3$, and $LiCOOCH_3$. The pH of the deionized water was adjusted using NH_4OH to pH 9 to prevent ion exchange with hydronium ions. For measurements of specimens submerged in a solution, the bottom ring of the test fixture was taped to the bottom of a 50 ml Petri dish containing the liquid. Membranes for strength measurements were grouped into two categories: electrochemical and static. Electrochemical membranes were operated in a d.c. cell described above at 60 °C for 16 h in their respective solutions, while static membranes were suspended in the same electrolyte solution in the d.c. cell without any potential being applied (except of course air, mineral oil and deionized water specimens, which were held in air/solution at 60 °C for 16 h in a drying oven). The biaxial fracture strength was calculated as [39]:

$$\sigma_f = \frac{3P}{2\pi t^2}\left[(1-\nu)\frac{D_S-D_L}{2D^2}+(1+\nu)\ln\left(\frac{D_S}{D_L}\right)\right] \tag{1}$$
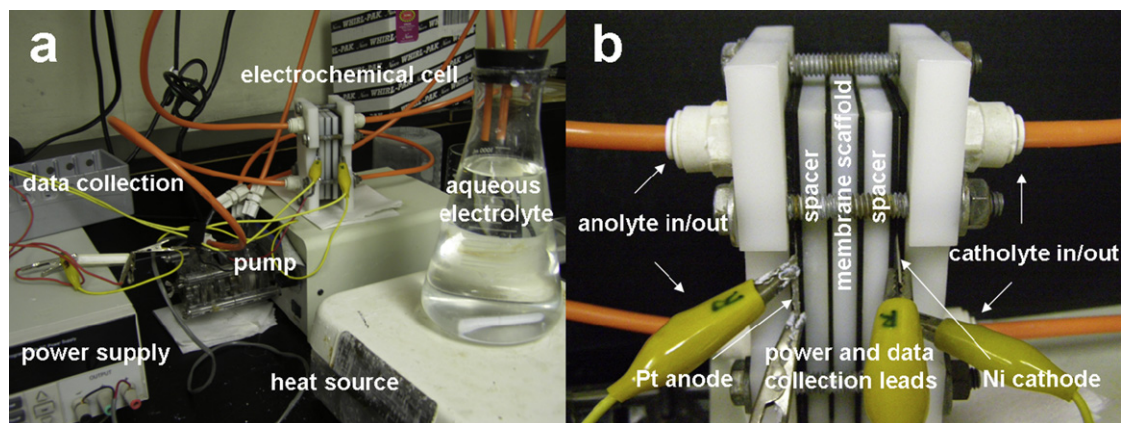
Fig. 1. Pictures of (a) electrochemical testing setup used for d.c. conductivity and electrochemical corrosion measurements, and (b) the cell apparatus used for electrochemical tests.

where P is the applied load, t is the specimen thickness, v is Poisson's ratio, D_S and D_L are the support and load ring diameters, respectively, and D is the specimen diameter. Additional electrochemical strength measurements were made in LiOH at 60 °C for 48 h according to Equation (1) to investigate the difference in strength between the anode and cathode side of the electrochemically-tested membranes.

3. Results

3.1. Physical properties

Phase purity of the as-received, high-purity LATP used for corrosion, strength, and electrochemical testing evaluated by XRD is depicted in Fig. 2. All specimens were confirmed to be of the $Li_{1.3}Al_{0.3}Ti_{1.7}P_3O_{12}$ rhombohedral structure with no detectible secondary phases. The relative density of samples, calculated by dividing the bulk density by the theoretical density, was between 95% and 96%. Fig. 3 is a representative SEM micrograph of the fracture and polished surfaces of a specimen, showing primarily intergranular fracture and a relatively fine microstructure [30].

3.2. Static corrosion results

Table 1 provides the measured corrosion rate for the LATP pellets soaked in saturated aqueous LiOH for the specified time periods at 65 °C or 105 °C. It is evident that from a mass change perspective, LATP would be considered extremely corrosion-resistant to LiOH. There is very little mass loss during the duration of the tests, and in one instance there is actually a slight gain in mass. This was confirmed to be the result of picking up Na via ion exchange to form sodium titanium phosphate (NTP) at the surface, as seen in the XRD pattern in Fig. 4. The depth of NTP formation was examined by XRD measurements after surface grinding soaked pellets, and was shown to be limited to the outside ~50 μm of the pellets. The micrographs also show no noticeable changes in the surface microstructure between a virgin pellet and the pellet soaked for 4 weeks in boiling LiOH. Also seen in the post-corrosion x-ray pattern is the fact that besides a slight shift from LATP to the sodium analogue, there does not appear to be any other secondary phases or decomposition of the LATP phase. Ion exchange is well known for NaSICON structures and Na^+ will exchange for Li^+ in LATP causing cracking due to volume expansion. This behavior of Na ion exchange into the LATP structure to form the sodium analogue always occurred in this study during tests involving aqueous solutions with some Na present, and will be examined in more detail in subsequent sections.

3.3. Ionic conductivity results

#### 3.3.1. A.c. conductivity

The Nyquist plot in Fig. 5 provides the interesting result that there is no significant change in the overall a.c. impedance behavior between a virgin pellet and one boiled in saturated LiOH for 4 weeks. However, there is a slight difference in the slope of the blocking electrode portion of the plot and slightly higher impedance at the junction of the grain boundary arc and the blocking electrode, evidence of the surface layer of NTP formed via ion exchange. This relatively unchanged a.c. impedance response of the bulk LATP, in conjunction with the lack of measurable mass-based corrosion, would lead one to believe that LATP is in fact stable in hot aqueous solutions of LiOH.

Impedance data of an LATP membrane tested under d.c. conditions (25 mA cm^{-2}) are shown in Fig. 6. At first glance it appears that there is a significant loss in conductivity as the test proceeds. However, this may be an artifact of the experimental procedure used. Materials in the NZP family show a tendency to hydrate and change their lattice parameters [40,41], and the membrane used for a.c. impedance measurements was thoroughly dried between each measurement, and thus the hydrated state was not tested. In Fig. 7 it is interesting to note that every time the membrane was dried, measured, and restarted there is an apparent 'break in' period of high voltage which eventually lowers and flattens out. This is most likely a re-hydration period, which results in the ionic conductivity matching what was recorded in the voltage and current during the flat regions. Impedance measurements, as conducted using this approach, were a poor predictor of d.c. performance.

3.3.2. D.c. conductivity

D.c. conductivity results in the aqueous Li salt solutions are summarized in Table 2. Each cell operated at a different voltage due to differing half–cell reactions at the anode and cathode, but in each case the potential across the LATP membranes was ~2 V. This condition, while more extreme than what might be seen in a typical battery system, was used to determine the stability of LATP in applications requiring high current density and allowed for rapid comparisons of stability between the various aqueous solutions. The calculated d.c. conductivities are in the range of 1.1–1.8 mS cm^{-1} for the different solutions tested. These values are much lower than the 2.4 mS cm^{-1} predicted by solid state a.c. impedance, in agreement with a previous test in LiOH [30]. Solid/liquid interfacial resistance to ion transfer lowers the conductivity and will undoubtedly be different between the solutions.

Fig. 8 provides a graph of the current density and voltage as a function of time for a representative run of each aqueous lithium
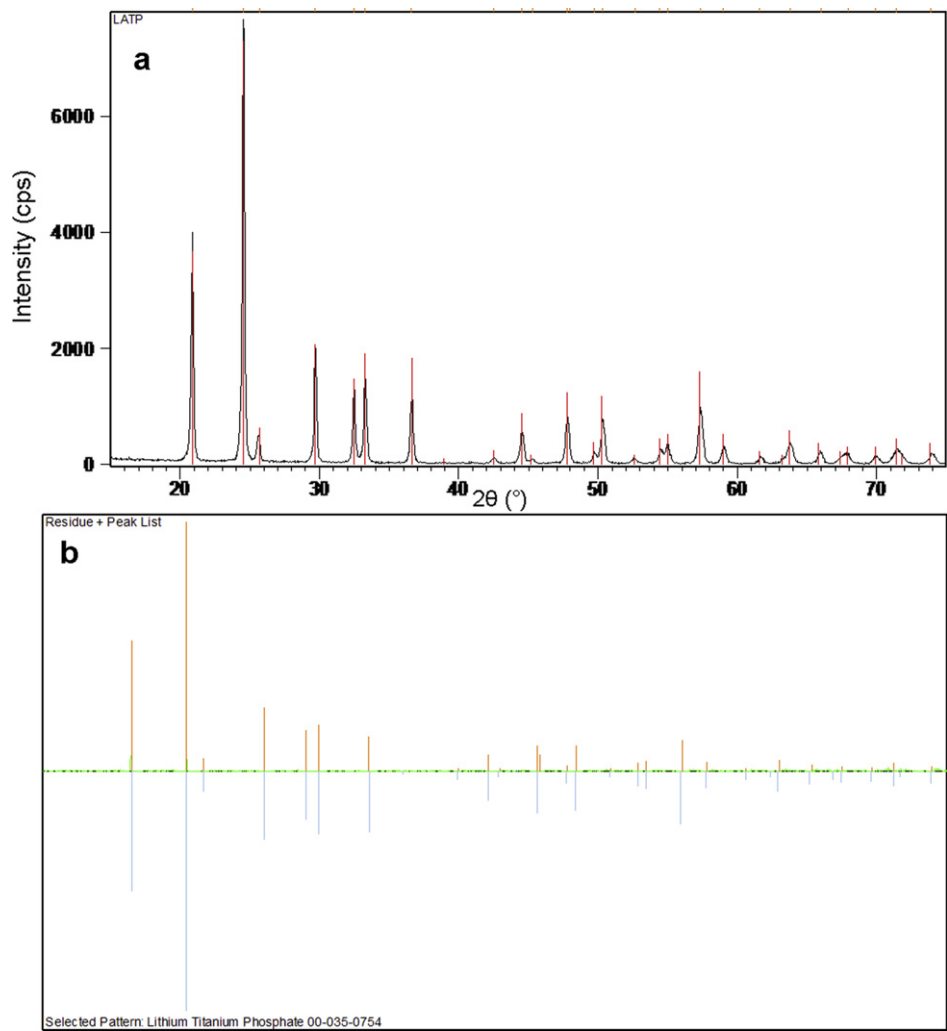
Fig. 2. XRD patterns of high-purity LATP showing a) peak intensity and profile and b) a comparison with an indexed LTP pattern with rhombohedral NZP crystal structure.
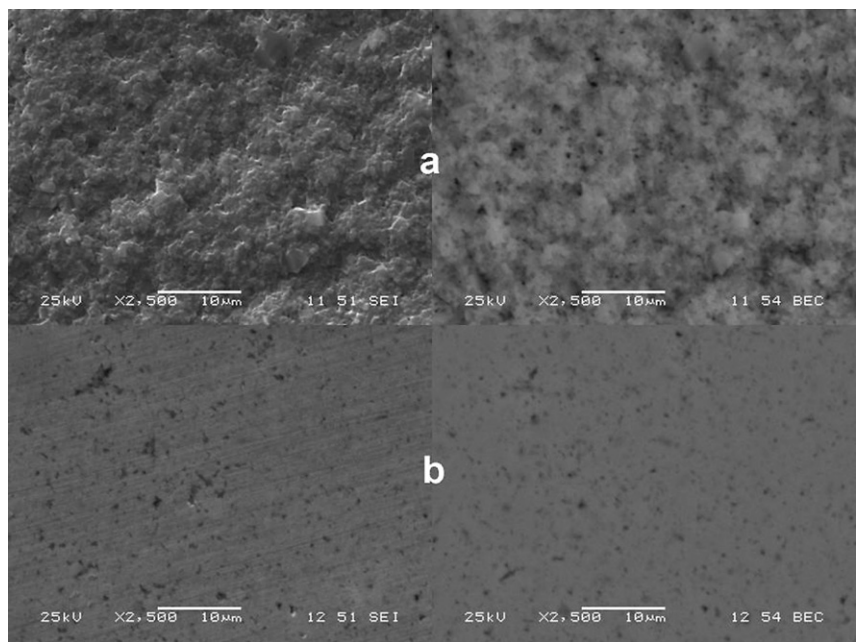
Fig. 3. Secondary (left) and backscatter (right) SEM images of (a) a fracture surface and (b) a polished cross section of high-purity LATP.

Table 1
Measured corrosion rate of LATP in saturated LiOH solution.

	Corrosion rate (mg cm^{-2} 100 h^{-1})		
	1 Week	4 Weeks	7 Weeks
$T = 65\ °C$	0.04 ± 0.02	0.03 ± 0.01	0.02 ± 0.01
$T \sim 105\ °C$	-0.03 ± 0.03	0.01 ± 0.02	NA

salt solution tested in a common flask scenario. Each cell was run for 30 h, after which the membrane was analyzed for any signs of degradation. Again, a clear 'break in' period of ∼4 h is seen regardless of the solution.

The factor that had the most dramatic effect on the integrity of the membrane was found to be the concentration of Na contamination. The membrane run in LiCl solution was cracked and flaking (Fig. 9) upon cell disassembly. ICP analysis results, summarized in Table 3, showed that the LiCl solution contained ∼220 ppm Na which was much higher than the other three solutions. The

degradation was confirmed as ion exchange by XRD analysis of failed membranes, showing significant formation of NTP (greater than that shown in Fig. 4) which has a larger unit cell volume and will cause lattice expansion and cracking if the material is rigidly confined, such as the cell apparatus used. To confirm this effect, a known amount of NaNO$_3$ was added into a LiNO$_3$ solution (identical to that previously used) to bring the Na$^+$ level up to ∼250 ppm and the same test was repeated. The membrane in this test failed in a similar manner to the original LiCl membrane and XRD again confirmed the formation of NTP. Fig. 9 shows EDS analysis of the polished cross section of the membrane run in LiNO$_3$ solution with ∼250 ppm Na, showing a clear Na-rich surface layer and slight gradient into the material. Indeed LATP proved extremely sensitive to ion exchange with Na, with detectable NTP formation after only 30 h of operation occurring even in the solutions with ∼10 ppm Na.

Membranes tested in LiOH showed degradation in the form of pitting and flaking on the cathode side of the membrane only, as
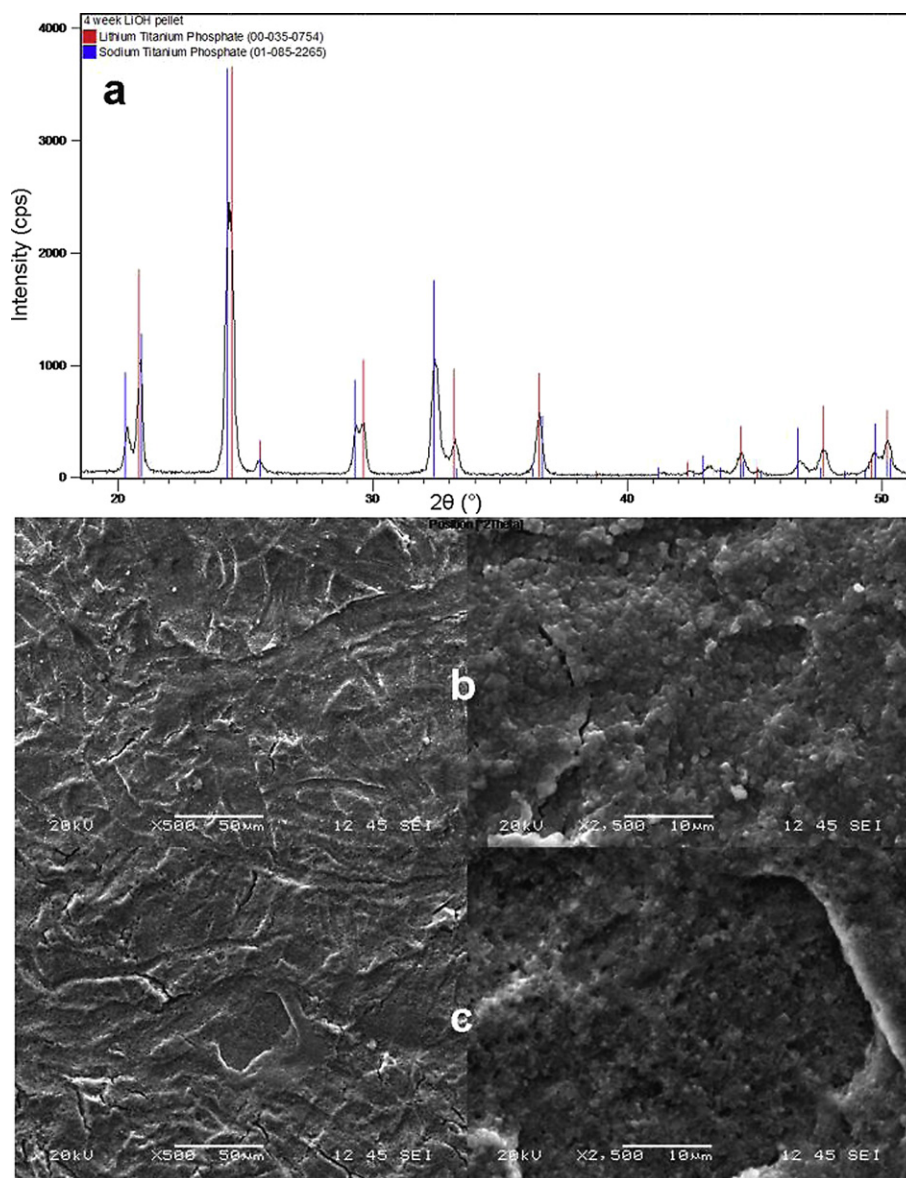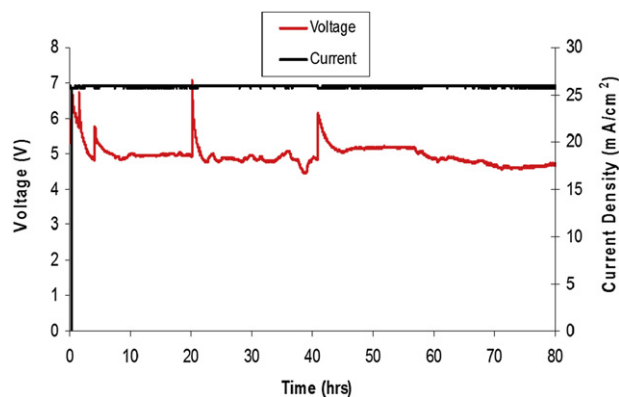

Fig. 4. Results of LiOH static corrosion showing (a) an XRD pattern showing NTP formation in LATP as a result of Na$^+$ ion exchange, and SEM images of the surface of (b) a virgin LATP pellet and (c) an LATP pellet after 4 weeks of exposure to boiling saturated LiOH.
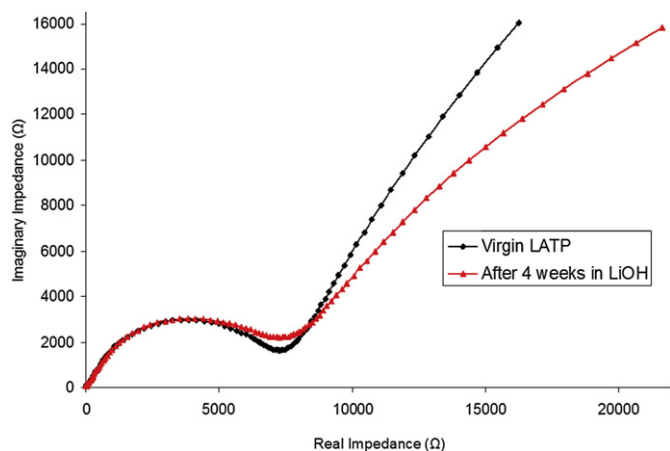
Fig. 5. Nyquist plot used to calculate the solid state a.c. conductivity of LATP before and after 4 weeks of exposure to boiling, saturated LiOH.

shown in Fig. 10. Subsequent runs confirmed this interesting result. In an effort to increase membrane longevity, a completely symmetric separate flask LiOH cell was run with Ni anode/cathode and the direction of current flow was manually switched every 24 h, causing the anode and cathode sides of the membrane to alternate. The

Fig. 6. Results of an LATP in aqueous $LiNO_3$ d.c. electrochemical cell showing (a) the change in a.c. conductivity as a result of an applied current of 25 mA cm^{-2} at 40 °C over time, and (b) Nyquist plots showing a change in the grain boundary conductivity.

Fig. 7. Voltage\current density versus time trace for an LATP membrane in aqueous $LiNO_3$ d.c. electrochemical cell used to measure the a.c. conductivity as a function of operation time at 25 mA cm^{-2} and 40 °C.

voltage and current traces for this run are given in Fig. 11, showing the cell was able to operate for 215 h, at which point the degradation on both sides of the membrane resulted in failure.
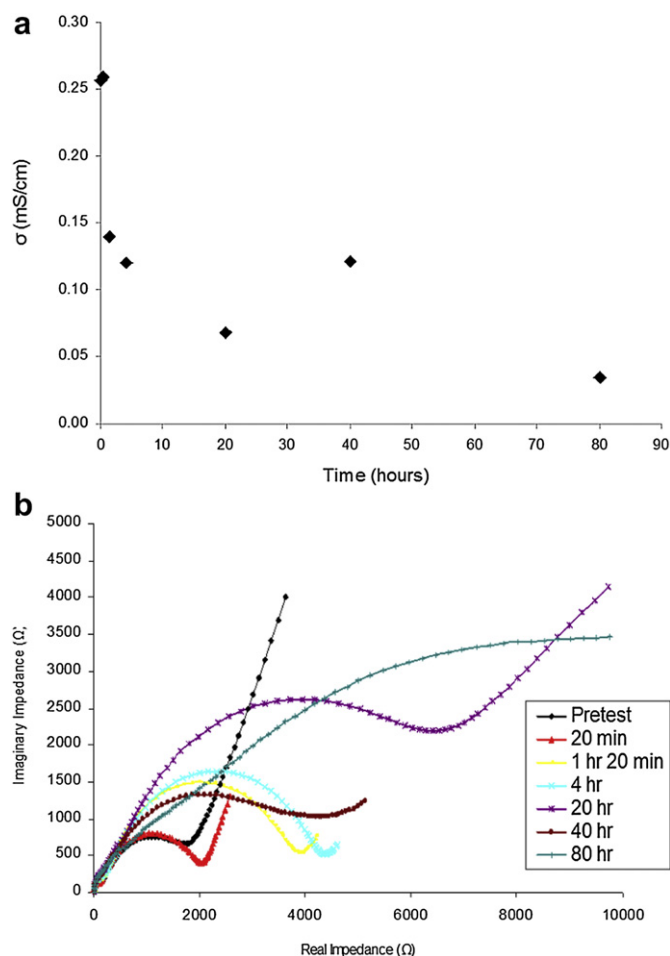
The $LiNO_3$ and $LiCOOCH_3$ systems did not fail and did not undergo any observable changes in physical appearance during the 30 h tests. Longer-term runs in these two chemistries were performed, the longest of which was 625 h of continuous operation without membrane failure in an aqueous $LiCOOCH_3$ solution and common flask configuration. The electrode reactions were such that a mole of acid and a mole of base were generated at the same rate, and therefore the solution was self-buffered at pH ~8. Upon disassembly the membrane was a slightly off-white color on the anode side, but there was no visible pitting or cracking and post-test analysis revealed only Na ion exchange consistent with other runs. Two other runs of >300 h of cell operation were performed in aqueous $LiNO_3$ in a common flask without membrane failure, but with slight formation of Li_3PO_4 on the anode side of the membrane. This formation was also detected during even short-term tests in LiCl solution, and in all cases appeared to form subsurface 'blisters', of which a severe case is shown in Fig. 12.

It appears that if the Na concentration in the aqueous electrolyte is kept low, cell longevity is strongly dependent on the pH of the aqueous solutions. The terminal pH of each solution under a common flask configuration is given along with the Na content in Table 3. Low pH leads to H$^+$ ion exchange in LATP (and other materials from the NZP family) and is well documented [36,42,43]. Instability in high pH, on the other hand, has not been as thoroughly addressed or understood. Using the separate flask and pH controlled separate flask configurations with $LiCOOCH_3$ solution, the effect of pH on cell longevity was investigated. Fig. 13 shows that when the compartments are kept separate and the anolyte and catholyte quickly become acidic and basic, respectively, the voltage rises quickly and the membrane fails. However, when the pH is maintained in the broad window of 6.5–11.5, cell longevity is greatly increased. This can then be compared with the self-buffered common flask run which lasted 625 h with no failure (only initial 325 h graphed for ease of comparison). The spikes in voltage at 75 and 110 h proved to be Li_2CO_3 scaling on the cathode electrode, which once removed resulted in low voltage.

Table 2
Membrane conductivity measured in d.c. electrochemical cells tested in a common flask configuration.

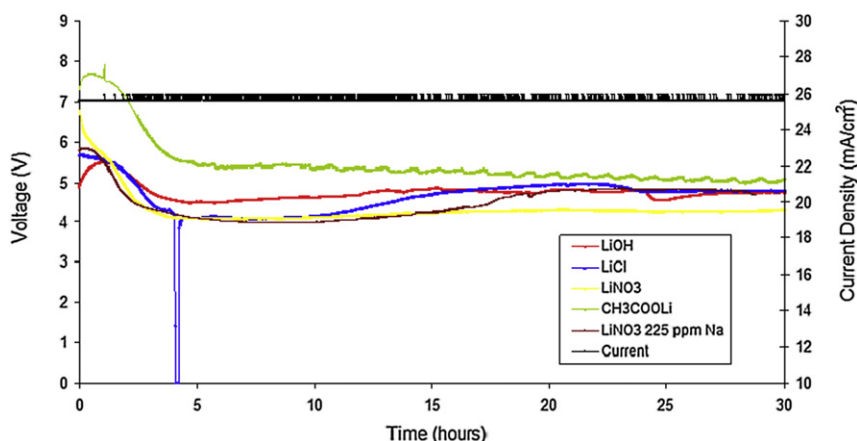|	LiOH	$LiNO_3$	$LiCOOCH_3$	LiCl
σ (mS cm^{-1})	1.7	1.8	1.1	1.5

Fig. 8. Voltage\current density versus time traces for LATP membranes in various aqueous Li salts with 25 mA cm^{-2} current density at 40 °C.

3.4. Strength results

Strength results are summarized in Tables 4 (static tests) and 5 (electrochemical tests). While the data are sparse, the results are quite surprising. The average biaxial strength measured for LATP was 144 MPa in air and 191 MPa in mineral oil. However, there is an 82% drop in strength to 26 MPa for LATP exposed to deionized water, despite no changes in the XRD patterns, mass, or impedance spectra. A comparison of static versus electrochemical tests showed little difference in LiNO$_3$ (35 versus 44 MPa) or LiCOOCH$_3$ (54 versus 46 MPa), with a strength decrease in LiOH (76 versus 49 MPa). The strength of LATP when exposed to aqueous solutions of Li salts varies, but is consistently much lower than the strength measured in air. Exposure to deionized water resulted in a much larger decrease in strength then the effects of operating in an electrochemical cell or being soaked in aqueous solutions of Li salts. When LATP was removed from the holder and dried to allow X-ray diffraction measurements, the samples were noticeably stronger. Measurements showed that the strength of the dried membranes increased from 26 MPa to 59 MPa, consistent with a dehydration reaction. It is important to note that membranes soaked and run electrochemically in LiCl solution cracked prior to strength measurements.

4. Discussion

The high-purity, fine-grained LATP had excellent strength (191 MPa) despite being microcracked [30] when tested in mineral

Fig. 9. Results from a d.c. electrochemical cell using an LATP membrane in aqueous LiCl at 25 mA cm^{-2} and 40 °C showing (a) cross-sectional EDS mapping of Na, and (b) a membrane cracked after short-term testing.

oil so as to exclude moisture from the crack tip. Using the measured fracture toughness of 1.1 MPa√m [30], the calculated flaw size is only 20 μm, suggesting good processing for this LATP. When exposed to air, the flaw size increased to 35 μm under the same test conditions. Exposure to water resulted in at least an order of magnitude increase in flaw size. Because XRD, a.c. impedance, mass change, and scanning electron microscopy were unable to detect any change, it is likely that a grain boundary glass containing P is being subjected to slow-crack growth under stress. Phosphate glasses are prone to stress-corrosion cracking [44,45], and strength is lowered at the crack tip in the presence of water, where the stress-enhanced chemical reactions are given as [46]:

$$H_2O + P-O-P \rightarrow 2(P-OH) \tag{2}$$

$$H_2O + P-O-M \rightarrow P-OH + M-OH \tag{3}$$

where M is a metal cation. Equations (2) and (3) show how water can react with the $P-O-P$ or $P-O-M$ bonds, resulting in crack propagation. In this way, a significant reduction in strength could occur while being nearly undetectable via mass change measurements or XRD analysis.

The trend of membrane strength in static solutions was LiCl $\ll$ H$_2$O < LiNO$_3$<CH$_3$COOLi < LiOH as shown in Table 4. Ion exchange of Na$^+$ for Li$^+$ caused cracking of the LATP in LiCl. Neither the pH of the solution nor the Na$^+$ content in the solutions correlate with the general trend in strength. One interesting observation is that the mechanical strength of LATP is highly correlated with the ratio of the concentration of salt divided by the maximum amount soluble at 40 °C. This ratio is 0.66, 0.36, and 0.12 for LiOH, LiCOOCH$_3$, and LiNO$_3$, respectively. The higher the ratio, the stronger the attraction of the water is to the ions in solution. If one assumes that deionized water has a ratio of 0, a plot of LATP strength as a function of this ionic strength ratio is surprisingly linear ($r^2 = 0.9997$). These data suggest that having highly solvated ions aids LATP strength in the pH range tested. An ICP test of the solutions showed no evidence of LATP solubility.

Table 3
Na concentration in aqueous lithium salt solutions measured by ICP.

	Deionized water	LiOH	LiNO$_3$	LiCOOCH$_3$	LiCl	LiNO$_3$ + NaNO$_3$
Na (ppm)	<1	11	5	13	223	256
pH at 40 °C	9.0	11.9	10.8	8.4	10.3	10.7
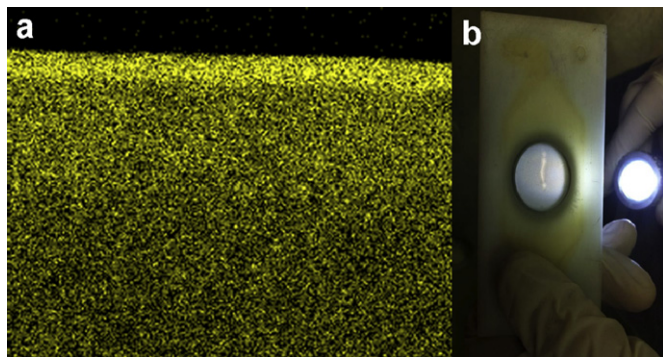
**Fig. 10.** Results from a d.c. electrochemical cell using an LATP membrane in aqueous LiOH at 25 mA cm^{-2} and 40 °C showing optical images of (a) anode and (b) cathode surfaces of the membrane after testing, and (c) an SEM comparison of anode and cathode surfaces with (d) a higher magnification image of pitting observed on the cathode side of the membrane.
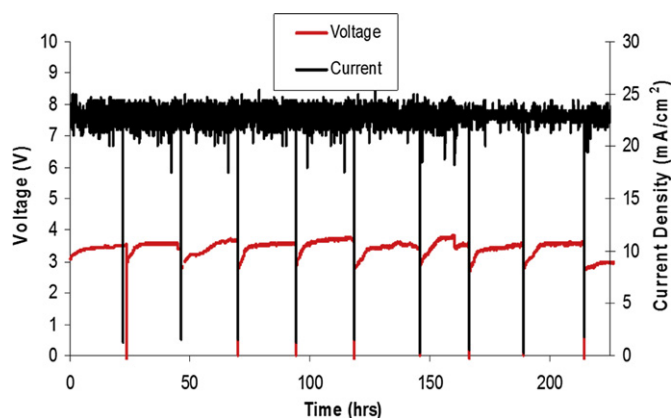
Fig. 11. Voltage\current density versus time trace for an LATP membrane in aqueous LiOH d.c. electrochemical cell at 25 mA cm^{-2} and 40 °C with the anode and cathode leads being reversed every 24 h.

It was anticipated that strength could be used to see electrochemical degradation. A comparison of Tables 4 and 5 show that there was no difference in strength between LATP exposed to the electrochemical driving force and those in the same solution, but without current passing through them for both LiNO$_3$ and LiCOOCH$_3$ solutions. This may be the result of the short duration of the tests, but the ability of LATP to be tested for hundreds of hours in LiCOOCH$_3$ supports these data. Also, since there is evidence of hydration/dehydration reactions, it is important that the LATP sample not be constrained in the test setup when being dehydrated or rehydrated in order to avoid cracking of the membrane due to the accompanying volume change.

The electrode reactions for all tests were predominantly water splitting reactions at the Pt anode and Ni cathode. For LiOH solutions they proceeded as in Equations (4) and (5):
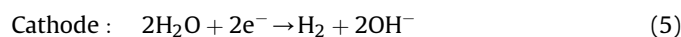
$$\text{Anode}: \quad 4OH^- \rightarrow O_2 + 2H_2O + 4e^- \tag{4}$$
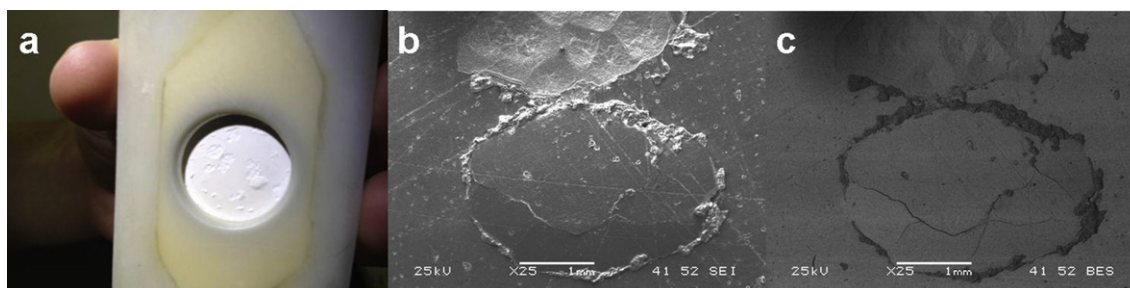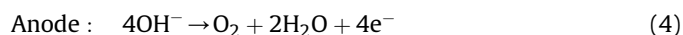
Fig. 12. Sub-surface Li$_3$PO$_4$ 'blisters' on the anode side of an LATP membrane seen in an (a) optical image, (b) Secondary SEM image, and (c) backscatter SEM image.
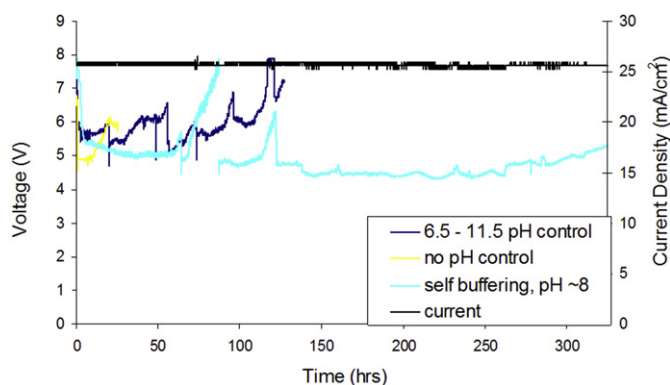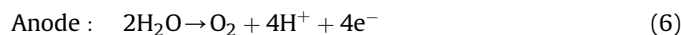
Fig. 13. Voltage\current density versus time traces for LATP membranes run in aqueous $LiCOOCH_3$ solutions of differing pH at 25 mA cm^{-2} and 40 °C.

$$\text{Cathode}: \quad 2H_2O + 2e^- \rightarrow H_2 + 2OH^- \tag{5}$$

while for the LiCl, $LiNO_3$, and $LiCOOCH_3$ solutions they were as in Equations (6) and (7):

$$\text{Anode}: \quad 2H_2O \rightarrow O_2 + 4H^+ + 4e^- \tag{6}$$

$$\text{Cathode}: \quad 2H^+ + 2e^- \rightarrow H_2 \tag{7}$$

For either case, the net reaction is:

$$2H_2O \rightarrow 2H_2 + O_2 \tag{8}$$

Equation (9) gives a competing reaction at the Pt anode for the LiCl system as:

$$\text{Anode}: \quad 2Cl^- \rightarrow Cl_2 + 2e^- \tag{9}$$

The cathodic reaction is the same as Equation (5), giving an overall reaction of:

$$2Cl^- + 2H_2O \rightarrow H_2 + Cl_2 + 2OH^- \tag{10}$$

While Equation (9) is a secondary anode reaction for the LiCl solution, it does explain why the solution pH gradually rises as the test proceeds due to the lack of sufficient acid being produced to balance the hydroxide. This rise in pH continues until the production of hydroxide at the cathode and its subsequent oxidation at the anode according to Equation (4) are in equilibrium. The electrode reactions in a common flask scenario for the $LiNO_3$ and $LiCOOCH_3$ solutions are of sufficient complexity as to not be discussed in detail here, but it can be said that a competing gas formation reaction at the Pt anode in the $LiNO_3$ solution allowed for an overall rise in pH until it became buffered in the same manner as LiCl, while the lack of such a reaction allowed the $LiCOOCH_3$ solution to remain buffered at pH ~8.

For the membranes exposed to LiOH under electrochemical conditions, noticeable strength degradation occurred. Additional strength measurements were made to test the difference in strength between the cathode and anode side of the membrane in support of observed degradation (pitting) on the cathode side.

Results supported the visual observations, with the strength when the cathode side was in tension being 61% lower on average than when the anode side was in tension. The reaction at the LiOH cathode produces hydroxyl ions, which are carried towards the cathode. One might expect attack at the surface of the LATP as opposed to the pitting which occurred, with fracture initiating within the sample as shown in Fig. 10.

Interestingly, high pH appears to have little effect statically, but under a potential it has a significant effect on the cathode (reducing) side of the membrane. This type of cathodic corrosion could be explained by a model recently proposed by Virkar [47–49], explaining that if the ionic and electronic currents through the membrane are in the same direction (which is the case for all electrochemical cells operated in this study), there is the possibility that the chemical potential of Li metal at the very surface of the membrane may be lower than that of a Li^+ ion during transport, causing local precipitation of Li at the membrane/electrolyte solution interface. This would lead to degradation consistent with the pitting observed on the cathode side of the membrane in LiOH cells. This is possible because there must be a non-zero concentration of free electrons and an accompanying local, non-zero electronic current in all solids at finite temperatures in order to satisfy the local equilibrium criterion [50,51]. Therefore, although LATP is predominately an ionic conductor with electronic conductivity several orders of magnitude lower than its ionic conductivity, there is still the possibility of electronic transport locally to provide electrons that could reduce lithium ions to lithium metal. Recently, this model has been supported experimentally in solid oxide electrolyzer cells [52].

This instability at high pH was also confirmed for the $LiNO_3$ system by running a separate flask cell with a LiOH anolyte and $LiNO_3$ catholyte, thus preventing acidic conditions at the anode while allowing the cathode to experience increasingly basic conditions. As the cell operated, LiOH was produced at the cathode and the catholyte pH changed from 7.6 to 11.3 over 72 h, resulting in advanced pitting only on the cathode side of the membrane identical to that seen in a LiOH cell.

However, the fact that Li^+ could be transported for hundreds of hours without any evidence of pitting for cells run in a pH range of 8–9 does not support this model, nor did SEM observations, which failed to find Li metal precipitated at any of the freshly fracture pits on the cathode side of the membrane. This may indicate that the solution pH has an effect on transport parameters and the chemical potential of Li ions versus Li metal.

Previous studies have suggested that NaSICON-type materials are unstable in water [42,43,45]. While NaSICON has been shown to have good stability in NaOH for long periods of time, this is the first study to suggest that LATP could be used in aqueous solutions if the pH could be controlled in a moderately basic pH range. While strength measurements show that water degrades the mechanical properties of this material to values lower than NaSICON, there is no indication that the degradation is catastrophic as long as ion exchange, which puts the anode side in compression and the cathode side of the membrane in tension, can be limited and the pH of the solution can be kept in the range of 7–10. Unfortunately, none of the salts tested satisfy this condition under desired operating conditions. For this reason, it is suggested that non-protonic organic solvents be tested when using LATP as a membrane material.

Table 4
Biaxial strength for LATP tested statically.

	Air	Deionized water, dried	Deionized water	Mineral oil	LiOH	LiCl	LiNO$_3$	LiCOOCH$_3$
Strength (MPa)	144 ± 13 (5)	59 ± 19 (4)	26 ± 7 (13)	191 ± 11 (4)	76 ± 19 (7)	0 (4)	35 ± 8 (4)	54 ± 12 (4)

Number of samples tested is given in parentheses.

Table 5
Biaxial strength for LATP after electrochemical testing.

	LiOH	LiOH (48 h)	LiOH (48 h)	LiCl	LiNO$_3$	LiCOOCH$_3$
Strength (MPa)	49 ± 10 (3)	41 ± 14 (A, 4)	17 ± 3 (C, 4)	0 (3)	44 ± 15 (3)	46 ± 4 (3)

Number of samples tested is given in parentheses. A = anode side in tension, C = cathode side in tension.

5. Conclusions

When tested at the same Li$^+$ concentration (2 wt%) and current density (25 mA cm^{-2}) at 40 °C in deionized water, LiNO$_3$ and LiOH solutions resulted in the highest conductivity in LATP membranes (∼1.8 mS cm^{-1}) while LiCl was slightly lower (∼1.5 mS cm^{-1}) and LiCOOCH$_3$ had the lowest conductivity (∼1.1 mS cm^{-1}). Electrode reactions resulted in high pH at the cathode and low pH at the anode, both of which are problematic for LATP. However, by using a common flask, which allowed for self-buffering in the case of LiCOOCH$_3$, it was possible to show that the LATP was stable over hundreds of hours of operation in the pH range of 8–9.

High-purity, fine-grained LATP [30] is susceptible to stress-corrosion cracking, with strength decreasing dramatically (191–26 MPa) when exposed to water. The strength in salt solutions was highly correlated with the ability of water to solvate the salt, with LiOH showing the highest strength (76 MPa) in static solutions. In the case of LiOH, static testing showed that LATP could last for hundreds of hours in the same high pH (>11.5) that resulted in short-term cathodic pitting in electrochemical testing. It was also shown that changes in strength can be a more sensitive indicator of degradation than XRD and a.c. impedance measurements, evidenced here by the results of LATP in aqueous LiOH solutions.

In order for LATP to be used in aqueous solutions in electrochemical cells, two conditions must be satisfied for low-temperature (40–60 °C operation): 1) the pH must be maintained in the range of 7–10, and 2) the Na$^+$ concentration must be kept low to avoid ion exchange. There are no practical applications for LATP in aqueous solutions, but strength testing in mineral oil suggests that it may be worthwhile to look at this material in non-protonic organic solvents used for electrochemical cells.

Acknowledgments

References

[1] J.W. Fergus, J. Power Sources 195 (2010) 4554.
[2] P. Knauth, Solid State Ionics 180 (2009) 911.
[3] N. Anantharamulu, K.K. Rao, G. Rambabu, B.V. Kumar, V. Radha, M. Vithal, J. Mater. Sci. 46 (2011) 2821.
[4] A.D. Pasquier, I. Plitz, S. Menocal, G. Amatucci, J. Power Sources 115 (2003) 171.
[5] K.T. Chau, Y.S. Wong, C.C. Chan, Energy Convers. Manag. 40 (1999) 1021.
[6] P.C. Frost, J. Power Sources 78 (1999) 256.
[7] P. Gifford, J. Adams, D. Corrigan, S. Venkatesan, J. Power Sources 80 (1999) 157.
[8] D.H. Doughty, P.C. Butler, A.A. Akhil, N.H. Clark, J.D. Boyes, J. Electrochem. Soc. Interface (2010) 49.
[9] T. Tanaka, K. Ohta, N. Arai, J. Power Sources 97-98 (2001) 2.
[10] W. Li, J.R. Dahn, D.S. Wainwright, Science 264 (1994) 1115.
[11] W. Li, J.R. Dahn, J. Electrochem. Soc. 142 (1995) 1742.
[12] H.Q. Yang, D.P. Li, S. Han, N. Li, B.X. Lin, J. Power Sources 58 (1996) 221.
[13] J. Kohler, H. Makihara, H. Uegaito, H. Inoue, M. Toki, Electrochim. Acta 46 (2000) 59.
[14] A. Eftekhari, Electrochim. Acta 47 (2001) 495.
[15] J.W. Lee, S.I. Pyun, Electrochim. Acta 49 (2004) 753.
[16] J.Y. Luo, W.J. Cui, P. He, Y.Y. Xia, Nat. Chem. 2 (2010) 760.
[17] C.M. Burba, R. Frech, Solid State Ionics 177 (2006) 1489.
[18] A.K. Padhi, K.S. Nanjundaswamy, J.B. Goodenough, J. Electrochem. Soc. 144 (1997) 1188.
[19] C. Delmas, A. Nadiri, J.L. Soubeyroux, Solid State Ionics 28 (1988) 419.
[20] G. Wang, L. Fu, N. Zhao, L. Yang, Y. Wu, H. Wu, Angew. Chem. Int. Ed. 46 (2007) 295.
[21] Y.G. Wang, Y.Y. Xia, Electrochem. Commun. 7 (2005) 1138.
[22] G.X. Wang, S. Zhong, D.H. Bradhurst, S.X. Dou, H.K. Liu, J. Power Sources 74 (1998) 198.
[23] N.C. Li, C.J. Patrissi, G.L. Che, C.R. Martin, J. Electrochem. Soc. 147 (2000) 2044.
[24] X.H. Liu, T. Saito, T. Doi, S. Okada, J. Yamaki, J. Power Sources 189 (2009) 706.
[25] N.V. Kosova, D.I. Osintsev, N.F. Uvarov, E.T. Devyatkina, Chem. Sustain. Dev. 13 (2005) 253.
[26] J.Y. Luo, Y.Y. Xia, Adv. Funct. Mater. 17 (2007) 3877.
[27] H. Wang, K. Huang, Y. Zeng, S. Yang, L. Chen, Electrochim. Acta 52 (2007) 3280.
[28] R.B. Shivashankaraiah, H. Manjunatha, K.C. Mahesh, G.S. Suresh, T.V. Venkatesha, J. Electrochem. Soc. 159 (2012) A1074.
[29] H. Aono, E. Sugimoto, Y. Sadaoka, N. Imanaka, G. Adachi, J. Electrochem. Soc. 136 (1989) 590.
[30] S.D. Jackman, R.A. Cutler, J. Power Sources 218 (2012) 65.
[31] A.V. Joshi, S. Balagopal, J. Pendelton, U.S. Patent 8,075,758 (2011).
[32] J.H. Gordon, S. Bhavaraju, U.S. Patent Application 20120103826 (2012).
[33] M. Cretin, P. Fabry, L. Abello, J. Eur. Ceram. Soc. 15 (1995) 1149.
[34] N. Imanishi, S. Hasegawa, T. Zhang, A. Hirano, Y. Takeda, O. Yamamoto, J. Power Sources 185 (2008) 1392.
[35] T. Zhang, N. Imanishi, Y. Shimonishi, A. Hirano, Y. Takeda, O. Yamamoto, N. Sammes, Chem. Commun. 46 (2010) 1661.
[36] S. Hasegawa, N. Imanishi, T. Zhang, J. Xie, A. Hirano, Y. Takeda, O. Yamamoto, J. Power Sources 189 (2009) 371.
[37] T. Zhang, N. Imanishi, Y. Shimonishi, A. Hirano, J. Xie, Y. Takeda, O. Yamamoto, N. Sammes, J. Electrochem. Soc. 157 (2010) A214.
[38] Y. Shimonishi, T. Zhang, N. Imanishi, D. Im, D.J. Lee, A. Hirano, Y. Takeda, O. Yamamoto, N. Sammes, J. Power Sources 196 (2011) 5128.
[39] ASTMC1499-09, Standard Test Method for Monotonic Equibiaxial Flexure Strength of Advanced Ceramics at Ambient Temperature, ASTM, Philadelphia, PA, 2009.
[40] J. Gulens, B.W. Hildebrandt, J.D. Canaday, A.K. Kuriakose, T.A. Wheat, A. Ahmad, Solid State Ionics 35 (1989) 45–49.
[41] J.D. Canaday, S.F. Chehab, A.K. Kuriakose, A. Ahmad, T.A. Wheat, Solid State Ionics 48 (1991) 113.
[42] P.G. Komorowski, S.A. Argyropoulos, R.G.V. Hancock, J. Gulens, P. Taylor, J.D. Canaday, A.K. Kuriakose, T.A. Wheat, A. Ahmad, Solid State Ionics 48 (1991) 295.
[43] R.O. Fuentes, F. Figueiredo, F.M.B. Marques, J.I. Franco, Solid State Ionics 139 (2001) 309.
[44] B.C. Bunker, G.W. Arnold, J.A. Wilder, J. Non-cryst. Solids 64 (1984) 291.
[45] Y.K. Lee, M. Tomozawa, J. Non-cryst. Solids 248 (1999) 203.
[46] T.I. Suratwala, R.A. Steele, G.D. Wilke, J.H. Campbell, K. Takeuchi, J. Non-cryst. Solids 263-264 (2000) 213.
[47] A.V. Virkar, J. Power Sources 172 (2007) 713.
[48] A.V. Virkar, Int. J. Hydrogen Energy 35 (2010) 9527.
[49] A.V. Virkar, J. Power Sources 196 (2011) 5970.
[50] A.V. Virkar, J. Power Sources 147 (2005) 8.
[51] A.V. Virkar, J. Electrochem. Soc. 138 (1990) 1481.
[52] M.A. Laguna-Bercero, R. Campana, A. Larrea, J.A. Kilner, V.M. Orera, J. Power Sources 196 (2011) 8942.